

ChemComm

Accepted Manuscript



This is an *Accepted Manuscript*, which has been through the Royal Society of Chemistry peer review process and has been accepted for publication.

Accepted Manuscripts are published online shortly after acceptance, before technical editing, formatting and proof reading. Using this free service, authors can make their results available to the community, in citable form, before we publish the edited article. We will replace this *Accepted Manuscript* with the edited and formatted *Advance Article* as soon as it is available.

You can find more information about *Accepted Manuscripts* in the [Information for Authors](#).

Please note that technical editing may introduce minor changes to the text and/or graphics, which may alter content. The journal's standard [Terms & Conditions](#) and the [Ethical guidelines](#) still apply. In no event shall the Royal Society of Chemistry be held responsible for any errors or omissions in this *Accepted Manuscript* or any consequences arising from the use of any information it contains.

Cite this: DOI: 10.1039/coxx00000x

www.rsc.org/xxxxxx

ARTICLE TYPE

New Six- and Seven- Membered Ring Pyrrole-Pyridine Hydrogen Bond Systems Undergoing Excited-State Intramolecular Proton Transfer

Zhiyun Zhang, Yen-Hao Hsu, Yi-An Chen, Chi-Lin Chen, Tzu-Chieh Lin, Jiun-Yi Shen and Pi-Tai Chou*

Received () XthXXXXXXXXXX 20XX, Accepted Xth XXXXXXXXXXXX 20XX

DOI: 10.1039/b000000x

New molecules, **6-HB** and **7-HB**, possessing six- and seven-membered ring pyrrole-pyridine hydrogen bond, respectively, are designed and synthesized, which undergo excited-state intramolecular proton transfer with distinct reaction dynamics.

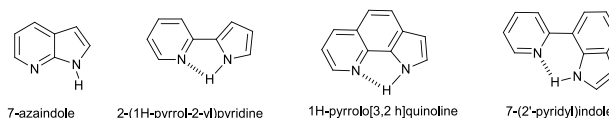
It is always fascinating to strategically design and synthesize molecules endowed with unique photophysical properties for probing the associated fundamental and applications. Among various anomalous types, those molecules exhibiting excited-state intramolecular proton transfer (ESIPT) and consequently rendering the large Stokes shifted emission have been receiving enormous attention. ESIPT molecules possess both proton donor and acceptor sites, from which the formation of intramolecular hydrogen-bond (H-bond) serves as the prerequisite for the translocation of the proton (or hydrogen atom) in the excited state.¹ The proton accepting site could be carbonyl oxygen, pyridyl nitrogen or azole-nitrogen, while hydroxyl, amino and occasionally pyrrolic groups serve as the proton donors.¹

Among various types of H-bonds, the pyridine-pyrrole pair is considered to be unique. This is mainly due to the fact that the pyrrolic N-H bond is rather directional compared with e.g., O-H bond that has more degrees of freedom to access H-bonding. Together with weak acidity of the pyrrolic proton, the pyrrole-pyridine H-bond formation may require optimized distance and orientation between pyrrole and pyridine. These prerequisite parameters may impose strong correlation among chemical structure, H-bond and the associated ESIPT dynamics.

Starting from a two-ring system fused by pyrrole and pyridine, molecules 7-azaindole (see Scheme 1) and its derivatives are the representatives. However, the highly steric 4-membered-ring configuration prevents the intramolecular H-bond formation and hence prohibits ESIPT. Alternatively, catalysed by the protic solvent molecules, 7-azaindole undergoes pyrrole N-H → pyridine proton transfer in the excited state, resulting in a prominent green tautomer emission.²

On the other hand, pyrrole and pyridine moieties could be linked by a single bond, forming 2-(1H-pyrrol-2-yl)pyridine (Scheme 1). 2-(1H-pyrrol-2-yl)pyridine possesses a weak five-membered ring H-bond so that slow ESIPT takes place via the thermally activated structural bending motion associated with the H-bond.³ As for the fused five membered ring H-bonding system such as 1H-pyrrolo[3,2-h]quinoline (Scheme 1), the intramolecular H-bond formation is restrained in terms of

orientation and distance and hence is weaker in strength. The lack of observing ESIPT for 1H-pyrrolo[3,2-h]quinoline (see Scheme 1) and its derivatives⁴ manifests that the fused aromatic framework is too rigid to fine-tune the H-bond. With respect to the six membered ring, pyrrolic-pyridine H-bonding system, Waluk and co-workers have reported the occurrence of ESIPT in a system of e.g. 7-(2'-pyridyl)indole⁵ (Scheme 1). This non-fused structure is relatively flexible, so that the structural bending motion associated with H-bonding strength plays a key role to account for ESIPT. Up to this stage, none of ESIPT has been reported for fused heterocyclic ring systems possessing six-member ring pyrrolic-pyridine H-bond. The fused, six membered-rings H-bond, from the chemical aspect, may be stronger than that of fused five-membered ring due to its favourable orientation and distance. Also, as for further extension, it is a great challenge as well as fundamental importance to search for pyrrole-pyridine ESIPT system possessing seven membered-ring H-bond, which, to our knowledge, is unprecedented.

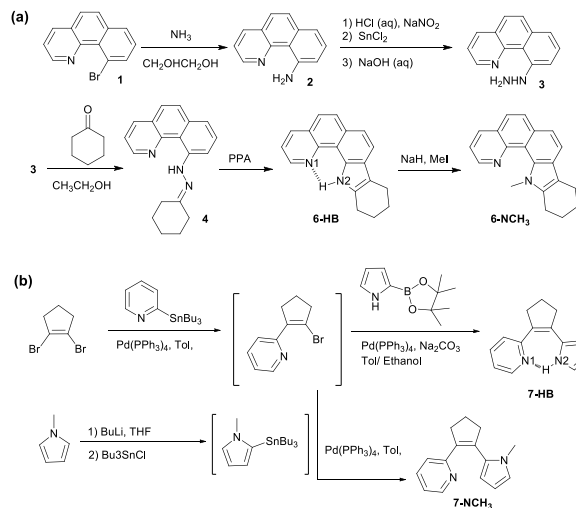


Scheme 1. Representative pyridine-pyrrole structures possess intramolecular H-bond, except for 7-azaindole. Note that various derivatives based on these parent molecules are not shown here.

We herein report on the design and syntheses of two new pyrrole-pyridine systems possessing six- and seven- membered ring intramolecular pyrrole-pyridine H-bond, namely 10,11,12,13-tetrahydro-9H-quinolino[8,7-a]carbazole (**6-HB**) and 2-(2-(1H-pyrrol-2-yl)-cyclopent-1-enyl)pyridine (**7-HB**) (Scheme 2). We then demonstrate that H-bonding distance/orientation imposed by the geometry constrain plays crucial role for the observed ESIPT dynamics.

As depicted in Scheme 2(a), synthesis of **6-HB** began with displacement of bromine of 10-bromobenzo[*h*]quinoline (**1**) by the amino group to afford benzo[*h*]quinolin-10-amine (**2**). Further reduction of the diazo-derivative of (**2**) by stannous chloride produced 10-hydrazinylbenzo[*h*]quinoline (**3**), followed by condensation with cyclohexanone, readily provide the corresponding hydrazine (**4**). Subsequent Fischer cyclization in polyphosphoric acid (PPA) smoothly delivered **6-HB** (~57%). In a separated route (b), 1,2-dibromocyclopent-1-ene was used as

the starting material, which then linked pyridine and pyrrole by sequential Still and Suzuki couplings, forming a novel seven membered ring H-bonding system, **7-HB** (~32%). For a fair comparison, the *N*-methyl derivatives of **6-HB** and **7-HB**, i.e., **6-NCH₃** and **7-NCH₃**, respectively (see Scheme 2), are also synthesised, which serve as the non-ESIPT model. It is also worthy to note that enormous efforts have been made to synthesize 1H-indolo[6,7-h]quinolone, which is considered to be the parent molecule of **6-HB** free from alkyl substituents at the pyrrole ring, but unfortunately failed at the last step of Fischer cyclization, due perhaps to the complicated rearrangement process, resulting in carboxyl-terminal fragments (see Scheme S1 of ESI†).



Scheme 2 Syntheses (a) **6-HB** and **6-NCH₃**, (b) **7-HB** and **7-NCH₃**.

Detail of synthetic route and characterization is provided in the ESI†. The growth of **6-HB** crystal is successful and the structure resolved by x-ray analysis is displayed in Fig. 1. Apparently, the fuse of three aromatic rings makes **6-HB** planar with the dihedral angle $\angle N(1)-C(13)-C(12)-C(11)$ of 0.18° ($\angle N(2)-C(11)-C(12)-C(13) \sim 0.31^\circ$). The $N(1) \cdots N(2)$ and $N(2)H \cdots N(1)$ H-bond distances are measured to be 2.782 and 2.193 Å, respectively. The latter is also supportive by the computation (B3LYP/6-311+G(d,p)/PCM, see ESI† for detail), estimating a H-bond distance of 2.173 Å. For comparison, we have synthesized an ESIPT molecule, **6-HBTs** (see Fig. 1), possessing a six membered ring H-bond between amino N-H and pyridine, for which the H-bond distance is measured to be 1.863 Å via x-ray analyses. Therefore, as for the fused six membered-ring H-bond system, the pyrrole-pyridine H-bond distance in **6-HB** is longer than the typical amino N-H...N (pyridine) H-bond distance (in **6-HBTs**). In yet another approach, a great effort has been made in growing single crystal of **7-HB** without success. Alternatively, the structure optimization of **7-HB** was done by the computational approach (see ESI† for detail). The result shown in Table S1 of ESI† clearly indicates that the three unfused rings in **7-HB** are virtually in a planar configuration owing to the formation of a seven membered ring H-bond and the H-bond distance is calculated to be as short as 1.789 Å.

Evidence for the intramolecular H-bond formation is also provided by the ¹H NMR data. With a similar type of chemical

structure the stronger intramolecular H-bond strength qualitatively correlates with the more downfield shift of proton NMR.⁶ As a result, the $N(2)-H \cdots N(1)$ proton signals of **6-HB** and **7-HB** in CDCl₃ were located at $\delta = 11.55$ and 13.96 ppm, respectively. The $\delta > 10$ downfield shift and sharp N-H peak supports the intramolecular H-bond formation for both **6-HB** and **7-HB**. This can be also evidenced by the IR frequencies of the N-H stretching vibrations of **6-HB** and **7-HB** observed at 3391 and 3360 cm⁻¹, respectively (Fig. S1 in ESI†). Empirically, ESIPT dynamics may correlate with the strength of the preexisting H-bond.⁷ This viewpoint is supportive by the corresponding spectroscopy and dynamics elaborated as follows.

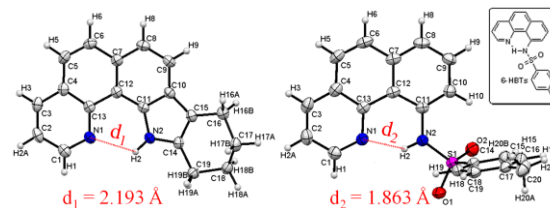


Fig. 1 The single crystal structures of **6-HB** (left) and **6-HBTs** (right). Insert: molecular structures of **6-HBTs**.

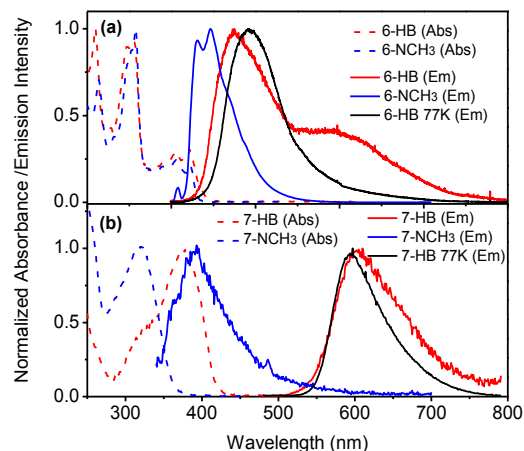


Fig. 2 The absorption (Abs, dish line) and emission (Em, solid line) spectra of (a) **6-HB** and **6-NCH₃**, and (b) **7-HB** and **7-NCH₃** in 60 cyclohexane at 295 K and 77K (frozen cyclohexane matrix).

The absorption and emission spectra of **6-HB** and **7-HB** in cyclohexane at room temperature are shown in Fig. 2. The absorption spectra of **6-HB** and **7-HB** show lowest lying peak at 365 and 378 nm, respectively, which can be assigned to the $\pi \rightarrow \pi^*$ transition, as is also supported by the frontier orbitals analyses shown in Table S1 (see ESI†). **7-HB** exhibits a large Stokes shifted emission maximized at 603 nm, whereas dual emission bands are resolved for **6-HB** with peak wavelengths at 436 and ~590 nm. In comparison, **6-NCH₃** and **7-NCH₃** were investigated, which respectively exhibit normal Stokes shifted emission at 400 and 395 nm (see Fig. 2). The results of these non-ESIPT models lead us to conclude the anomalous emission for **6-HB** (~590 nm) and **7-HB** (603 nm) to be the proton-transfer tautomer emission resulting from ESIPT. Also noted is the significant blue shifted absorption in **7-NCH₃** (cf. **7-HB**), indicating a loss of planarity hence π -conjugation for **7-NCH₃** due to the lack of intramolecular H-bond stabilization.

Despite the sameness regarding the occurrence of ESIPT, the difference lies in the dual emission for **6-HB** that is in sharp contrast to solely proton-transfer emission in **7-HB**, manifesting the distinct ESIPT dynamics. Fig. 3(a) and 3(b) show the femtosecond fluorescence upconversion data for **6-HB** and **7-HB**, respectively. Upon monitoring at the normal emission region of 450 nm, the time-dependent emission profile of **6-HB** consists of a system-response-limited rise component (< 150 fs), followed by a single-exponential decay component, for which the lifetime fitted to be 1.4 ± 0.2 ps. On the other hand, the time-dependent tautomer emission monitored at 620 nm, shows a rise component of 1.3 ± 0.2 ps, accompanied by a population decay time of 3.8 ± 0.2 ps. The rise of tautomer emission, within experimental error, is identical with the decay time of the normal emission, establishing a precursor-successor ESIPT relationship. As for **7-HB**, upon monitoring at the tautomer emission peak of 600 nm, the temporal evolution consists of a system-response-limited rise (< 150 fs) followed by a population decay time of 33 ± 0.3 ps.

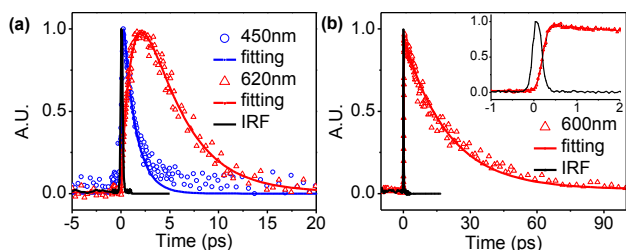


Fig. 3 The femtosecond time-resolved fluorescence spectra of (a) **6-HB**, and (b) **7-HB** in cyclohexane at 295 K. Inset: (b) in the short time scale of 2 ps.

We also performed deuterium substitution of the pyrrolic proton for **6-HB** and **7-HB**, denoted as **6-DB** and **7-DB**, respectively, and measured their ESIPT dynamics. As shown in Fig. S2 of ESI† the decay (1.5 ± 0.2 ps for normal emission) and rise (1.4 ± 0.3 ps for tautomer emission) for **6-DB**, within experimental error, are the same as that of **6-HB**. The nearly deuterium isotope independent reaction kinetics indicates that ESIPT for **6-HB** is not induced by the N-H stretching, but rather via certain structure bending motions associated with the changes of H-bond distance/angles. For **6-HB** such a bending motion may be subject to substantial barrier due to the rigidity of its fused arenes framework. For a fair comparison, Waluk and co-workers report a six membered ring H-bond system 7-(2'-pyridyl)indole (see Scheme 1), which is structurally more flexible (cf. **6-HB**) and undergoes barrierless type of ultrafast ESIPT reaction.^{5,8} Because the H-bond strength is about the same between 7-(2'-pyridyl)indole ($\delta_{\text{N-H}} = 11.37$ ppm)⁹ and **6-HB** ($\delta_{\text{N-H}} = 11.55$ ppm) in the ground state, the distinct ESIPT dynamics thus results from the structure flexibility (7-(2'-pyridyl)indole) versus rigidity (**6-HB**). This viewpoint is further supported by **7-HB** and its deuterium substitution **7-DB**. As for **7-DB** the rate of ESIPT is still too fast to be resolved with current upconversion system (> 150 fs)⁻¹ see Fig. S2). For **7-HB** (or **7-DB**) the non-fused and hence flexible structure, together with a strong H-bond (vide supra), make geometry readjustment facile, resulting in a barrierless type of ESIPT.

Further support for barrier (**6-HB**) versus barrierless (**7-HB**) type of ESIPT is provided by the cryogenic measurement (see Fig. 2), in which ESIPT is prohibited for **6-HB** in the 77 K

cyclohexane matrix, resulting in a unique 460 nm normal emission, whereas solely 600 nm tautomer emission is resolved for **7-HB**. Detailed temperature-dependent study is not feasible due to the restriction of current fluorescence upconversion setup. Alternatively, in a qualitative manner, we then made attempts to gain insight into the energy barrier of **6-HB** via the computational approach. In this approach the geometries of **6-HB** in the S_1 excited state were optimized (CAM-B3LYP/6-31+G(d,p), see ESI†) under the constraint of N(2)-H distance varied from 1.0 to 2.0 Å with an increment of 0.1 Å to map out the reaction potential energy surface (PES). The PES shown in Fig. S3 (see ESI†) indicates that the proton transfer from N(2)-H to N(1), i.e., from normal to tautomer form, in the S_1 state is associated with a non-negligible barrier of 2.3 kcal/mol. Conversely, the full geometry optimization of N(2)-H normal form for **7-HB** in the S_1 state (the Franck-Condon state) spontaneously relaxes to the N(1)-H tautomer form. Though qualitative, the computation result draws the similar conclusion for barrier (**6-HB**) versus barrierless (**7-HB**) type of ESIPT.

Summarization of ESIPT for **6-HB** and **7-HB** is depicted in Fig. 4. It is noteworthy that most ESIPT-type tautomer emission in the red gives low emission yield. This is mainly due to the nonradiative deactivation via those overtone vibrations associated with hydrogen-bonding motion.^{1b} **6-HB** and **7-HB** fit this category, in which the tautomer emission of **7-HB** is determined to be 1.6×10^{-3} , and is even lower for **6-HB**, being only 1.1×10^{-4} in cyclohexane. The lower yield for **6-HB** can be further rationalized by the poor overlap between HOMO and LUMO orbitals of the tautomer form (Table S1), giving a weak oscillator strength ($f \sim 0.03$). This viewpoint is supported by the small $S_1 \rightarrow S_0$ radiative decay rate constant k_r , calculated to be 2.9×10^7 s⁻¹ for the **6-HB** tautomer emission.

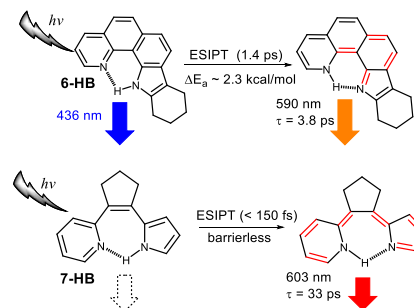


Fig. 4 The proposed mechanism of ESIPT **6-HB** and **7-HB**.

In conclusion, the above results demonstrate for the first time the pyrrole-pyridine ESIPT systems extended to six (fused rings) and seven membered ring H-bond. The unique feature of pyridine-pyrrole H-bond, manifested by its orientation and distance, effectively influences their ESIPT dynamics, hence the emission spectra, which are highly valuable for the further design of relevant ESIPT systems suitable for optoelectronic application.

Notes and references

Department of Chemistry, Center for Emerging Material and Advanced Devices National Taiwan University, Taipei, Taiwan, R.O.C.; E-mail: chop@ntu.edu.tw (P.-T. Chou)

† Electronic Supplementary Information (ESI) available: CCDC 1013475 and 1013476. For ESI and crystallographic data in CIF or other electronic format see DOI: 10.1039/b000000x/

1. (a) J. E. Kwon and S. Y. Park, *Adv. Mater.*, 2011, **23**, 3615; (b) A. P. Demchenko, K.-C. Tang and P.-T. Chou, *Chem. Soc. Rev.*, 2013, **42**, 1379.
2. C. A. Taylor, M. A. El-Bayoumi and M. Kasha, *Proc. Natl. Acad. Sci.*, 1969, **63**, 253.
3. (a) W.-S. Yu, C.-C. Cheng, Y.-M. Cheng, P.-C. Wu, Y.-H. Song, Y. Chi and P.-T. Chou, *J. Am. Chem. Soc.*, 2003, **125**, 10800; (b) M. Kijak, Y. Nosenko, A. Singh, R. P. Thummel and J. Waluk, *J. Am. Chem. Soc.*, 2007, **129**, 2738.
4. (a) A. Kyrychenko, J. Herbich, F. Wu, R. P. Thummel and J. Waluk, *J. Am. Chem. Soc.*, 2000, **122**, 2818; (b) J. Waluk, *Acc. Chem. Res.*, 2003, **36**, 832; (c) A. Kyrychenko and J. Waluk, *J. Phys. Chem. A*, 2006, **110**, 11958.
5. (a) G. Wiosna, I. Petkova, M. S. Mudadu, R. P. Thummel and Waluk, J., *Chem. Phys. Lett.*, 2004, **400**, 379; (b) Y. Nosenko, G. Wiosna-Salyga, M. Kunitski, I. Petkova, A. Singh, W. J. Buma, R. P. Thummel, B. Brutschy and J. Waluk, *Angew. Chem. Int. Ed.*, 2008, **47**, 6037.
6. T.-Y. Lin, K.-C. Tang, S.-H. Yang, J.-Y. Shen, Y.-M. Cheng, H.-A. Pan, Y. Chi and P.-T. Chou, *J. Phys. Chem. A*, 2012, **116**, 4438.
7. M.-W. Chung, J.-L. Liao, K.-C. Tang, C.-C. Hsieh, T.-Y. Lin, C. Liu, G.-H. Lee, Y. Chi and P.-T. Chou, *PCCP*, 2012, **14**, 9006.
8. A. L. Sobolewski and W. Domcke, *J. Phys. Chem. A*, 2007, **111**, 11725.
9. M. S. Mudadu, A. Singh and R. P. Thummel, *J. Org. Chem.*, 2006, **71**, 7611-7617.